RADC-TR-72-119
TECHNICAL REPORT
APRIL 1972

EFFECTS OF TURBULENCE INSTABILITIES ON LASER PROPAGATION

RCA LABORATORIES

SPONSORED BY
ADVANCED RESEARCH PROJECTS AGENCY
ARPA ORDER NO. 1279

ROME AIR DEVELOPMENT CENTER
AIR FORCE SYSTEMS COMMAND
GRIFFISS AIR FORCE BASE, NEW YORK

58

UNCLASSIFIED
Security Classification

DOCUMENT CONTROL DATA - R & D

(Security classification of title, body of abstract and indexing annotation must be entered when the overall report is classified)

1. ORIGINATING ACTIVITY (Corporate author) RCA Laboratories Princeton, New Jersey	2a. REPORT SECURITY CLASSIFICATION Unclassified 2b. GROUP N/A

3. REPORT TITLE

EFFECTS OF TURBULENCE INSTABILITIES ON LASER PROPAGATION

4. DESCRIPTIVE NOTES (Type of report and inclusive dates)
Quarterly Progress Report No. 3 9 December 1971 - 8 March 1972

5. AUTHOR(S) (First name, middle initial, last name)
David A. de Wolf

6. REPORT DATE April 1972	7a. TOTAL NO. OF PAGES 39	7b. NO. OF REFS 11
8a. CONTRACT OR GRANT NO. F30602-71-C-0356 b. PROJECT NO. ARPA 1279 c. Program Code 1E20 d.	9a. ORIGINATOR'S REPORT NUMBER(S) PRRL-72-CR-12 9b. OTHER REPORT NO(S) (Any other numbers that may be assigned this report) RADC TR-72-119	

10. DISTRIBUTION STATEMENT

11. SUPPLEMENTARY NOTES Monitored by: Lt. Darryl P. Greenwood (315) 330-3443; RADC (OCSE) GAFB, NY 13440	12. SPONSORING MILITARY ACTIVITY Advanced Research Project Agency 1400 Wilson Blvd. Arlington, VA 22209

13. ABSTRACT

Several statistics of the focal spot of a focussed laser beam in turbulent air are computed. The average area is recomputed for horizontal propagation, and corrected graphs are presented. Comparison to the half-power area is made, and it is concluded that the irradiance-weighted radius variance is a slightly better criterion, although the differences are small. The calculations are extended to slant paths. The power spectrum of the area scintillation is shown to be proportional to that of angle of arrival of a ray. It is computed for frozen flow and for random flow with zero mean velocity. Both spectra are initially flat, then decay as $f^{-2/3}$. A composite formula is suggested for the general case.

DD FORM 1 NOV 68 1473

Ia

UNCLASSIFIED
Security Classification

14. KEY WORDS	LINK A		LINK B		LINK C	
	ROLE	WT	ROLE	WT	ROLE	WT
Wave propagation Turbulent atmosphere, air Laser beam, focussed Optics, atmospheric Irradiance fluctuations						

EFFECTS OF TURBULENCE INSTABILITIES ON LASER PROPAGATION

DAVID A. de WOLF

CONTRACTOR: RCA LABORATORIES
CONTRACT NUMBER: F30602-71-C-0356
EFFECTIVE DATE OF CONTRACT: 9 JUNE 1971
CONTRACT EXPIRATION DATE: 8 JUNE 1972
AMOUNT OF CONTRACT: $49,990.00
PROGRAM CODE NUMBER: 1E20

INVESTIGATOR: DR. DAVID A. de WOLF
PHONE: 609 452-2700 EXT. 3023

PROJECT ENGINEER: LT. DARRYL P. GREENWOOD
PHONE: 315 330-3443

This research was supported by the Advenced Research Projects Agency of the Department of Defense and was monitored by Lt. Darryl P. Greenwood, RADC (OCSE), GAFB, N.Y. 13440 under contract F30602-71-C-0356.

Ic

FOREWORD

This Quarterly report was prepared by RCA Laboratories, Princeton, New Jersey under Contract No. F30602-71-C-0356. It describes work performed from 9 December 1971 to 8 March 1972 in the Communications Research Laboratory, Dr. K. H. Powers, Director. The principal investigator and project engineer is Dr. D. A. de Wolf.

The report was submitted by the author on 7 April 1972. Submission of this report does not constitute Air Force approval of the report's findings or conclusions. It is submitted only for the exchange and stimulation of ideas.

The Air Force Program Monitor is Lt. Darryl P. Greenwood.

PUBLICATION REVIEW

This technical report has been reviewed and is approved.

Darryl P. Greenwood
RADC Project Engineer

ABSTRACT

Several statistics of the focal spot of a focussed laser beam in turbulent air are computed. The average area is recomputed for horizontal propagation, and corrected graphs are presented. Comparison to the half-power area is made, and it is concluded that the irradiance-weighted radius variance is a slightly better criterion, although the differences are small. The calculations are extended to slant paths. The power spectrum of the area scintillation is shown to be proportional to that of angle of arrival of a ray. It is computed for frozen flow and for random flow with zero mean velocity. Both spectra are initially flat, then decay as $f^{-2/3}$. A composite formula is suggested for the general case.

SUMMARY

Atmospheric turbulence causes the focal spot of a focussed laser beam to scintillate, i.e., the irradiance distribution in the focal plane varies irregularly. In the first quarter of the contract period (9 June to 8 September 1971), a simple calculation of the variance of an irradiance-weighted radius of the focal spot was presented. It yielded an average focal-spot area equal to the sum of the diffraction-limited area and an area proportional to $L^3\kappa_m^{1/3}C_n^2$ (L = range, κ_m = microscale wavenumber, C_n^2 = refractive-index structure constant).

There exist arguments whether such a variance represents an effective area as well as the half-power area in the focal plane. Moreover, some numerical errors crept into the analysis and the graphs. Hence, the entire matter is presented again in Section I with errors rectified, and with a considerable discussion of the "differing" definitions of effective focal-spot area. We conclude that the differences are unimportant, and that the irradiance-weighted variance is more proper.

In Sections II and III, the analysis is extended to slant paths, ground-to-air, and air-to-ground. The theory summarized by Wyngaard, et al.[5] is utilized for incorporating the height dependence of $C_n^2(z)$ into the theory. The effects are much less than in ground-level horizontal propagation, and weakest for the ground-to-air case. Graphs are presented that allow one to convert the horizontal-propagation parameters into slant-path equivalents, when altitude of laser or receiver is known.

In Section IV, the power spectrum of focal-spot radius scintillation is computed. It is proportional to the power spectrum of angular fluctuations of a ray. We compute the latter for two cases: (i) Taylor's hypothesis, i.e., frozen flow with a steady wind velocity, and (ii) random velocity distribution with zero mean. An approximate formula is constructed for the composite of these two cases: it yields a spectrum that is a function of a square velocity $v^2 = U_T^2 + 16\Delta U^2/3$. Here, U_T is the mean-velocity component across the beam, and ΔU^2 is the velocity variance. The spectrum is flat when $\omega < v/L_o$ (ω is the angular frequency variable of the spectrum, L_o is the macroscale). It decays as $\omega^{-2/3}$ for $v/L_o < \omega < \kappa_m v$, and cuts off quite sharply when ω exceeds $\omega_m v$.

TABLE OF CONTENTS

LIST OF ILLUSTRATIONS

I. HORIZONTAL PROPAGATION PATH

In the First Quarterly Report[1], a formula was derived for the effective focal-spot radius r_L of a focussed laser beam propagating through turbulent air characterized by strength C_n^2 and scales $\ell_o \approx 5.92/\kappa_m$ and L_o. The definition of r_L is

$$r_L^2 = \int d^2\rho\ \rho^2 \langle I(\vec{\rho},L)\rangle \Big/ \int d^2\rho\ \langle I(\vec{\rho},L)\rangle \tag{1}$$

hence it is an average-irradiance weighted variance of the distance in the focal plane from the central axis. The result we obtained is

$$r_L^2 = (L/kr_o)^2 + 1.3\ L^3\kappa_m^{1/3}C_n^2 \tag{2}$$

for a Gaussian beam. The general result is

$$r_L^2 = r_{Lo}^2 + 1.3\ L^3\kappa_m^{1/3}C_n^2 \tag{3}$$

where r_{Lo} is defined by (1) if $\langle I(\vec{\rho},L)\rangle$ is replaced by the free-space $I_o(\vec{\rho},L)$. The result (2) is essentially the same as that of Varvatsis and Sancer[2].

Lutomirski and Yura[3] define another effective focal-spot radius r_L' ($z\theta$ in their notation) which is defined as a half-power radius such that $\langle I(\vec{\rho},L)\rangle = 1/2\ \langle I(0,L)\rangle$ for $\rho = r_L'$. They obtain

$$\begin{aligned} r_L' &\approx 0.9\ L^{3/2}\kappa_m^{1/6}C_n \quad \text{for } 0.4k^2L\ell_o^{5/3}C_n^2 \gg 1 \\ &\approx 0.7L^{8/5}k^{1/5}C_n^{6/5} \quad \text{for } 0.4k^2L\ell_o^{5/3}C_n^2 \ll 1 \end{aligned} \tag{4}$$

There is also a lower bound on L for the second criterion in (4) but it is of the order of one or several meters for systems with apertures of at least 10 cm diameter, and hence not of much practical importance.

The results (3) and (4) appear different for L less than $(0.4k^2\ell_o^{5/3}C_n^2)^{-1}$, a distance of roughly 7 km at 0.6 μm and more than 2000 km at 10.6 μm. This difference thus appears to manifest itself in practical situations, particularly in the infrared regime. At the time of writing - early 1972 - there appears to be disagreement among workers in the field about relevance and applicability of results (3) and (4). The purpose of this section is to clarify the matter.

The peculiarity of result (3) is the following: for truncated beams - particularly for the so-called Airy-disk case - one finds $r_{Lo} = \infty$, hence $r_L = \infty$.

and the result appears meaningless. Moreover, $r_L^2 - r_{Lo}^2$ depends on the microscale ℓ_o (or κ_m^{-1}).

The peculiarity of result (4) lies in the somewhat arbitrary definition of r_L' as a half-power radius,* and the dependence of r_L' upon the macroscale L_o.

We wish to make a case for the statements that result (3) is more fundamental than result (2) - also in the case that $r_{Lo} \to \infty$ - and that the difference between $(r_L^2 - r_{Lo}^2)^{1/2}$ and r_L' is rather small for all practical cases.

In order to do so, it is first noted that the definitions of $(r_L^2 - r_{Lo}^2)^{1/2} \equiv r_{LB}$, and $1.25\, r_L'$ coincide when $0.4k^2 L \ell_o^{5/3} C_n^2 \gg 1$. The reason is that the irradiance profile at $z = L$ has become Gaussian in which case the half-power radius differs from the irradiance-weighted variance by only a numerical factor ~ 1.25.

The next point is that (3) is a very general result, as noted on page 9 of Reference[1]. In Appendix I, we give a derivation well-known in radio astronomy[4] where an analogous problem exists in analyzing the power spectrum of backscattered radio pulses. The spectrum is a convolution of the spectra of the target scattering amplitude and the pulse envelope. Hence the variance width of the spectrum (which tells you something about the Doppler content of the astronomical object viewed) is the Pythagorean sum of the variance widths of the two component spectra in the convolution. The variance width of a square-pulse spectrum is infinite. Hence the analogy. The difficulty is circumvented by regarding the difference of the variances which can be computed in any practical case by exploiting the finite bandwidth of the observed spectrum. In our case, that means that $r_{LB}^2 = r_L^2 - r_{Lo}^2$ can be computed in practice because r_{Lo} is not really infinite: it is limited by finite signal-to-noise ratios and if these are taken into account *consistently* for r_L *and* r_{Lo} there is no real difficulty. I.e., one computes from the data,

$$r_L^2 = \int_0^{\rho_n} d^2\rho\ \rho^2 \left[\langle I(\vec{\rho},L) \rangle - I_o(\vec{\rho},L) \right] \Big/ \int_0^{\rho_n} d^2\rho\ \langle I(\vec{\rho},L) \rangle \qquad (5)$$

where ρ_n is a value of the radius beyond which the patterns vanish into noise. If the broadening due to turbulence occurs well within ρ_n, i.e., if the result of the above calculation yields $r_{LB} \ll \rho_n$, then it follows that the denominator of (5) is adequate since it is essentially equal to the total power emitted by the laser. It is quite true that the second ρ-moments of $\langle I(\vec{\rho},L) \rangle$ and $I_o(\vec{\rho},L)$ are proportional to ρ_n, but their *difference* is not. The quantity r_{LB}^2 therefore can be calculated and has meaning even when the variance width r_{Lo}^2 of the vacuum irradiance pattern is infinite. The irradiance pattern is thus broadened in turbulent air by convolution with the Fourier transform $I_B(\vec{q})$ - see Appendix I - of the mutual-coherence function of a spherical wave field in turbulent air divided by the equivalent vacuum field. The quantity r_{LB}^2 is simply the variance width of this Fourier-transform pattern $I_B(\vec{q})$, where $\vec{q} = (k/L)\vec{\rho}$.

*However, definition (II) of Ref. 1 yields essentially the same result (private communication, D. P. Greenwood).

In my opinion this settles the question of whether the resulting broadening should depend upon the macroscale L_o or upon the microscale ℓ_o. The broadening is clearly determined by the shape of $I_B(\vec{q})$. The variance width r_{LB}^2 of $I_B(\vec{q})$ is finite and therefore clearly a valid measure of the width. It is given by (A-10), hence it is a function of the *microscale*. It is fairly easy to understand why the broadening depends more essentially upon the microscale. The definition of $I_B(\vec{q})$ in (A-3) makes it perfectly clear that the radius parameter $\vec{q} = (k/L)\vec{\rho}$ of the Fourier-transform pattern in the focal plane is the Fourier-conjugate variable of the difference coordinate $\Delta\vec{\rho}$ in $< B(1)B^*(2)>$ Consequently the behavior of $I_B(\vec{q})$ for *large* q is determined by the *small* $\Delta\rho$-behavior of $< B(1)B^*(2)>$. These are both therefore determined by the *microscale* ℓ_o. On the other hand, the *macroscale* L_o determines the behavior of $< B(1)B^*(2)>$ for large $\Delta\rho$, hence of $I_B(\vec{q})$ for *small* q.

What we are saying is in effect that the half-power radius r_L' is not really a good measure of the broadening (although we will show further on that it isn't bad either). Remember that the pattern $< I(\vec{\rho},L)>$ in the focal plane is a convolution of $I_o(\vec{\rho},L)$ with $I_B(\vec{\rho},L) = I_B(\vec{q})$. When I_B is broad compared to I_o, obviously the broadening is given by $r_{LB}^2 \sim L^3\kappa_m^{1/3}C_n^2$ and the first criterion for r_L' given in (4) must hold. When I_B is *narrow* compared to I_o the broadening is also given by $r_{LB} \sim L^3\kappa_m^{1/3}C_n^2$, but this quantity is then small compared to the width of the main lobe of I_o, and therefore not interesting. The interesting case is when r_{LB} is comparable to the main-lobe width in which case Lutomirski and Yura[3] utilize $r_L' \sim L^{8/5}k^{1/5}C_n^{6/5}$ and the second criterion in (4). At infrared frequencies, most propagation paths of interest fall into this case when $C_n^2 \sim 10^{-13}m^{-2/3}$. What happens in this case is that the nulls between main lobe and side lobes of I_o are rapidly filled. The total patterns $< I>$ given in [3] indicate this at paths L larger than several hundred meters ($L = 100\ z_c$). The half-power radius then becomes rather arbitrary.

There is another way to examine this difference between r_L' and r_{LB}. It is simply to compare them! In fact, let us compare r_{LB} and $1.25\ r_L'$ to each other, since these coincide for a Gaussian beam.

$$\frac{1.25\ r_L'}{r_{LB}} \approx \frac{L^{8/5}k^{1/5}C_n^{6/5}}{L^{3/2}\kappa_m^{1/6}C_n} = \left(\kappa_m^{-5/3}k^2L\ C_n^2\right)^{1/10} \tag{6}$$

For fixed frequency, this ratio varies with $(LC_n^2)^{1/10}$, i.e., very weakly. Clearly, the definitions are not very different. More serious, however, is the restriction of validity of the numerator of (6) to the condition (p. 1657 of[3]),

$$10 < 0.4k^2L\ L_o^{5/3}\ C_n^2 < 10^4 \tag{7}$$

for errors of less than 25%. By taking the 10-th root of (7), we obtain

$$1.4(\kappa_m L_o)^{-1/6} < 1.25 r_L' / r_{LB} < 2.8(\kappa_m L_o)^{-1/6} \qquad (8)$$

A typical large surface value for $\kappa_m L_o$ is 10^3, hence we note that in the region of validity of the expression for r_L', we have

$$0.4 < 1.25 r_L' / r_{LB} < 0.9 \qquad (9)$$

Relationships (6) and (9) indicate clearly that there is not much numerical difference between r_L' and r_{LB} in the region of validity of the cited expression for r_L'. On the other hand, the expression for r_{LB} is valid over a wider range. Hence it is concluded that (3) is to be preferred to (4), although careful use of (4) does not lead to appreciable differences.

Horizontal propagation is characterized by constant C_n^2 along the propagation path. It is therefore fairly simple to plot (3) for this case. Figures 1 and 2 of Reference[1] contain some inaccuracies, hence new graphs are supplied in this report.

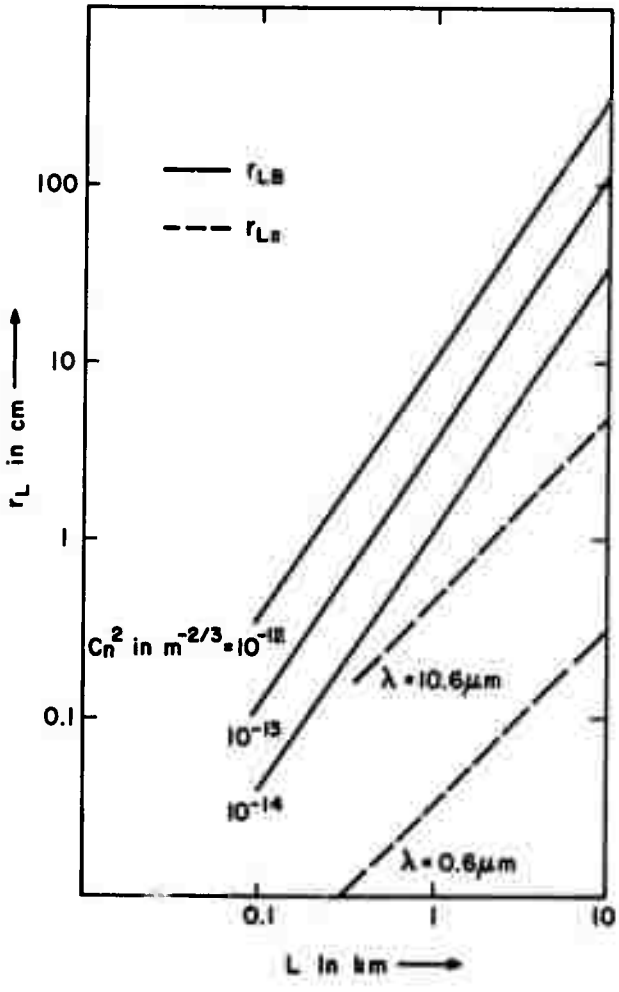

Figure 1.

The free-space focal-spot radius r_{Lo}, and its average broadening r_{LB} ($< r_L^2 > = r_{Lo}^2 + r_{LB}^2$) as functions of range L for $10^{-14} < C_n^2$ in $m^{-2/3} < 10^{-12}$.

In Figure 1, we plot r_L vs L according to (3). The solid lines represent r_{LB}, the second term in the right-hand side of (3). The dashed lines represent r_{Lo} for two different frequencies.

In Figures 2 and 3, we plot r_{oc} vs L. The critical laser aperture r_{oc} is defined to be such that $r_{Lo} = r_{LB}$. If r_{oc} is increased, then r_{Lo} is decreased and $r_L \sim r_{LB}$. That indicates that larger apertures than those with radius r_{oc} will not yield smaller average focal areas: a lower limit πr_{LB}^2 masks the diffraction area. By setting $r_{Lo} = L/kr_{oc}$ equal to r_{LB} we obtain

$$r_{oc} = 1/1.4\ kL^{1/2}\ \kappa_m^{1/6}\ C_n = L/kr_{LB} \tag{10}$$

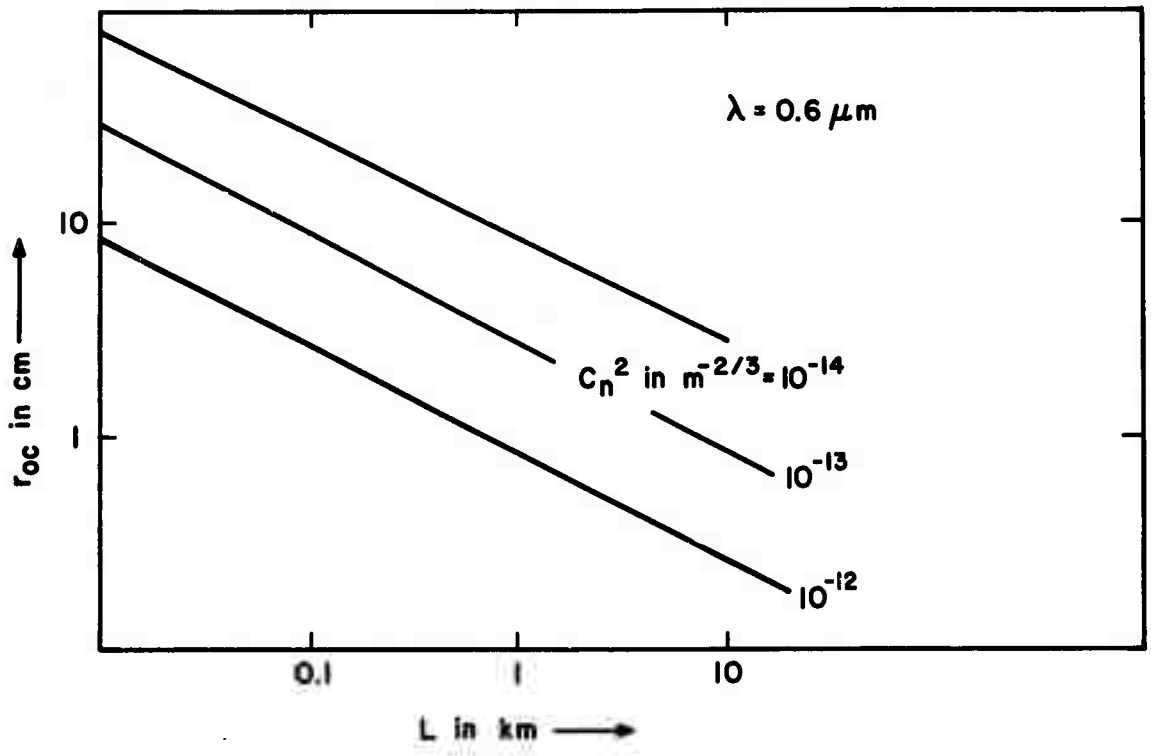

Figure 2. Maximal aperture radius r_{oc} required to obtain a minimal average focal-spot area as a function of range L for $10^{-14} < C_n^2$ in $m^{-2/3} < 10^{-12}$ at $\lambda = 0.6$ μm.

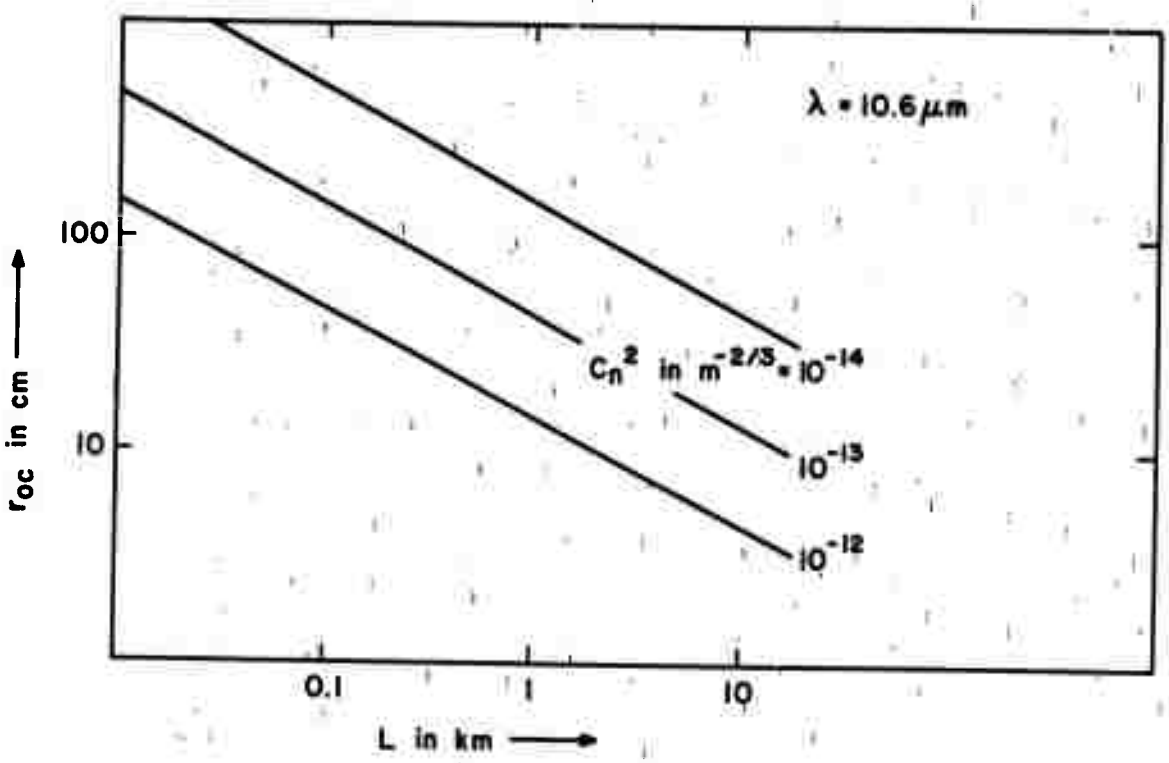

Figure 3. Maximal aperture radius r_{oc} required to obtain a minimal average focal-spot area as a function of range L for $10^{-14} < C_n^2$ in $m^{-2/3} < 10^{-12}$ at $\lambda = 10.6$ μm.

II. SLANT-PATH PROPAGATION: GROUND-TO-AIR

In this section, we will modify (3) for the case of slant-path propagation in which case C_n^2 is a function of altitude. To do so, we note that the main difference with horizontal propagation is that instead of obtaining in (A-10) a factor

$$L\epsilon^2 \int_0^\infty dKK^3\Phi(K)$$

from the limit $p \to 0$ in (A-9), we should be obtaining

$$\lim_{\rho\to 0} \left\{ 4\rho^{-2} \int_0^L ds\epsilon^2(s) \int_0^\infty dKK\Phi(K)[1 - J_o(K\rho s/L)] \right\} \tag{11}$$

$$= \int_0^L ds\epsilon^2(s)\ (s/L)^2 \int_0^\infty dKK^3\Phi(K)$$

for a slant path characterized by a path parameter s. Equation (11) inserted into (A-10) yields

$$r_{LB}^2 = 3.9\ L^2\kappa_m^{1/3} \int_0^L ds(s/L)^2\ C_n^2(z) \tag{12}$$

In adapting (12) to a situation where the laser is located at an altitude z_o close to the ground and pointed upwards at an elevation angle of θ with the horizon towards an object at distance L, it is noted that path coordinate s is related to altitude z through $s = (z-z_o)/\sin\theta$.

The behavior of $C_n^2(z)$ with altitude is fairly complicated - particularly at altitudes above 1 km. The Hufnagel curve, Figure 4, indicates the difficulties: occurrence of random disturbed layers and dependence of lower-altitude C_n^2 upon time of day. Wyngaard, et al. have surveyed recent developments in altitude dependence of C_n^2[5]. Their results yield,

$$C_n^2(z) = C_n^2(z_o)(T_o/T)^2(z_o/z)^{2/3}(1+z/\ell_s)^{-2/3}$$

$$\times \exp[-2(z-z_o)/h]\ , \tag{13}$$

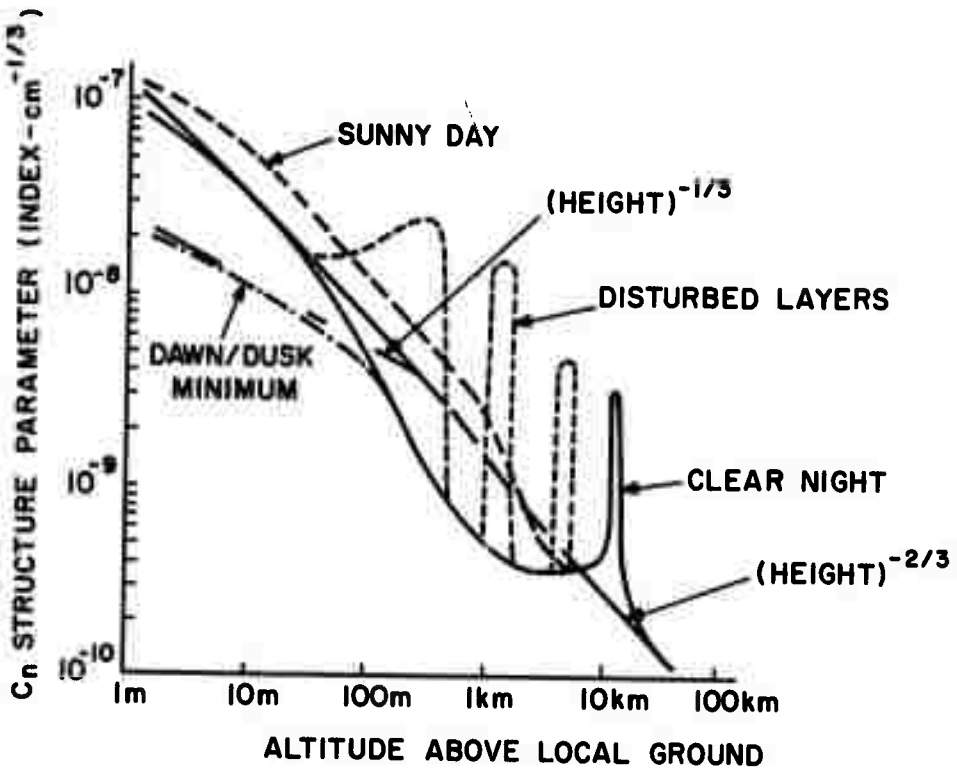

Figure 4. $C_n(z)$ in $cm^{-1/3}$ vs altitude z; the "Hufnagel curve". The Wyngaard, et al. predictions [Reference 5] are included.

where T is the temperature at altitude z (T_o at z_o), h is the scale-height of pressure at sea level (h ≈ 8.3 km), and ℓ_s is a length parameter related to the Monin-Obukhov length L_{MO} by $\ell_s = -L_{MO}/7$. This model predicts (for $2z << h$).

$C_n^2 \propto z^{-4/3}$ sunny day - midday (ℓ_s 1.5 m)

$C_n^2 \propto z^{-2/3}$ dawn, dusk ($\ell_s \to \infty$),

and Figure 4 bears the prediction out quite well. The older Fried model, cited by Titterton[6], and Sutton[7] will therefore not be followed. Note that Equation (12) is a function only of the receiver altitude $Z = L\sin\theta$, and that it can be rewritten as

$$r_{LB}^2(Z) = r_{LB}^2(0).F(Z)$$

$$F(Z) = \frac{3}{Z}\int_{z_o}^{Z} dz\, \exp(-2z/h)(z/Z)^2 \qquad (14)$$

$$\times\ (1+z/z_o)^{-2/3}[1+(z+z_o)/\ell_s]^{-2/3}$$

Note that the temperature dependence on altitude has been ignored. It is variable, but weak compared to the other s-dependent parameters in the F(Z) factor of (14). Certain approximations simplify the calculation of (14):

(i) *sunny day - midday situation*: We may replace the last two factors in (14) by $(z_o\ell_s)^{2/3}\,(z)^{-4/3}$ provided $Z >> z_o, \ell_s$. For $Z << z_o$ we obtain $F(Z) = 1$. The critical altitude Z_c for which $Z_c = z_o, \ell_s$ is of the order of 1 m or less when $z_o \approx 1$ m, and $L > 1$ km. Hence, slant paths are handled easily for most non-zero angles θ by means of this simplification.

(ii) *dawn, dusk situation*: Because $\ell_s \to \infty$ in this case, we replace the last two factors in (14) by $(z/z_o)^{-2/3}$ under the proviso that $Z >> z_o$, which is always true for any airborne target under consideration.

The remainder of this section is devoted to straightforward numerical expression of (14). It is easily seen from (10) and (14) that

$$r_{oc}(Z)/r_{oc}(0) = r_{LB}(0)/r_{LB}(Z) = [F(Z)]^{-1/2}. \qquad (15)$$

Hence, it suffices to plot (15) as a function of Z in order to infer the slant-path quantities from those at zero altitude for an equivalent path of length L.

(i) *sunny day - midday*: With the previously discussed simplifications, it follows that

$$F(Z) \sim 1.8\,[(z_o\ell_s)^{1/2}/Z]^{4/3} \text{ for } Z << h/2$$

$$\sim 0.85\, h^{5/3}(z_o\ell_s)^{2/3}/Z^3 \text{ for } Z >> h/2, \qquad (16)$$

the intermediate regime is governed by the incomplete gamma function from which (16) is derived.

(ii) *dawn, dusk*: Likewise, we obtain

$$F(Z) \sim 1.3(z_o/Z)^{2/3} \qquad \text{for } Z << h/2$$
$$\sim 0.7\, h^{7/3} z_o^{2/3}/Z^3 \qquad \text{for } Z >> h/2. \tag{17}$$

In our view, the Z >> h/2 forms in (16) and (17) should not be regarded very seriously because they depend upon validity of the model (13) above z = h/2 ∿ 4 km, and that is certainly above the altitudes where this model is valid.

In Figure 5, we plot the Z << h/2 forms of $[F(Z)]^{-1/2}$ vs Z, using $\ell_o \approx z_o \approx 1$ m. The plots are substantially the same as those in the Second Quarterly Report (9 September - 8 December 1971, sequel to Reference[1]). However, it is simpler to plot the ratios as functions of altitude Z, and to modify the horizontal-path results of Figures 1 to 3 by these altitude factors when the image at the end of path L is at altitude Z.

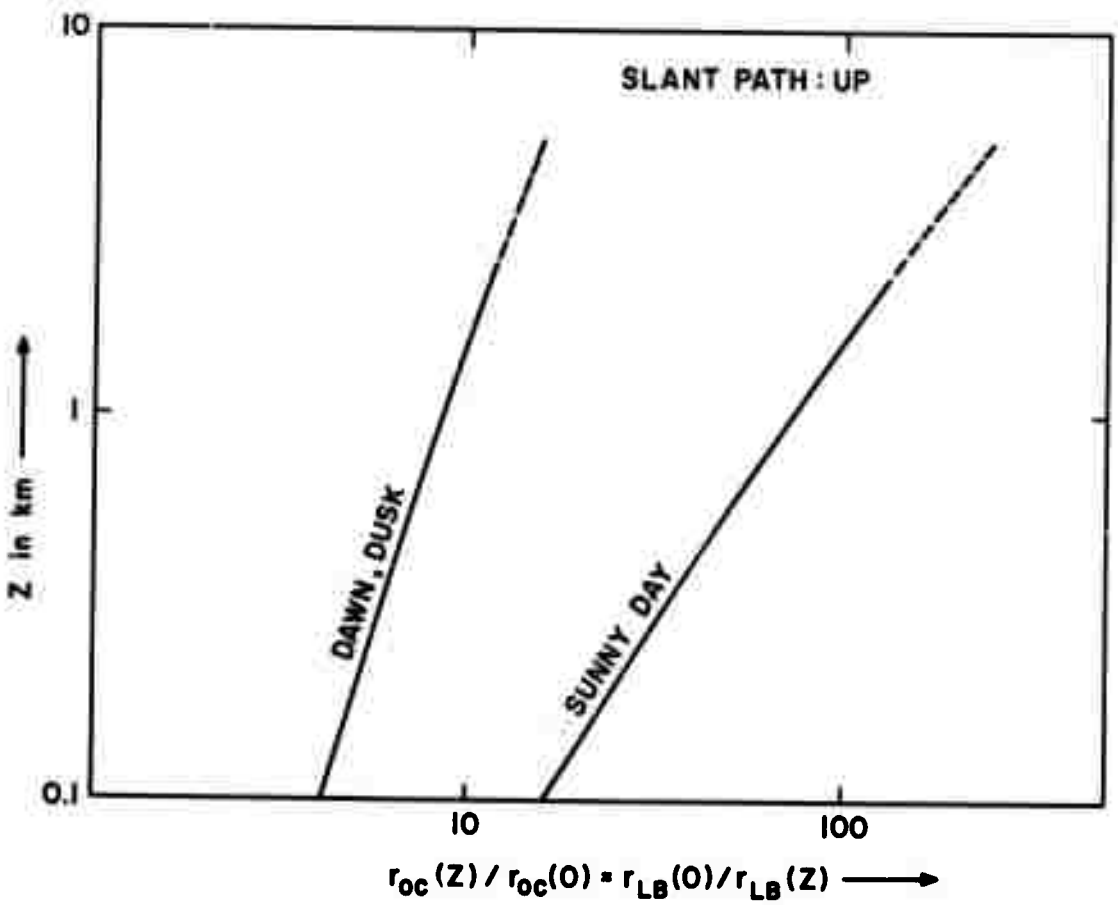

Figure 5. Modification factors for r_{Lo} and r_{oc} (from Figures 1 to 3) for ground-to-air propagation for laser transmitters at altitude Z.

Clearly, the effect of turbulence is much less pronounced on slant paths. It should be stressed that the curves in Figure 5 depend on $z_o^{1/3}$ and on $\ell_s^{1/3}$, and that we have chosen $z_o \approx 1$ m, $\ell_s \approx 1$ m. The slant-path results of Figure 5 should be scaled accordingly, if different values for z_o (laser height) and $\ell_s (= -L_{MO}/7)$ are utilized. Note that $Z = L \sin \theta$; these curves are functions only of the product $L \sin \theta$. Each point describes a variety of path-lengths L and elevation angles θ subject to $L \sin \theta = Z$.

III. AIR-TO-GROUND PROPAGATION

If it is the transmitter that is at an altitude z = Z, and the receiver at $z = z_o$ such that the propagation path has a length L at an inclination of $-\theta$ with the horizon (ignoring curvature effects), then a slightly different calculation ensues. Instead of (12), we obtain

$$r_{LB}^2 = 3.9\, L^2 \kappa_m^{1/3} \int_0^L ds(1 - s/L)^2\, C_n^2(z) \tag{18}$$

Because the dominant part of the integral is in the first 150 m or so above the ground, where $(1-s/L)^2 \approx 1$ for altitudes Z of 500 m or more, and because the model for $C_n^2(z)$ is not trustworthy above several hundred meters, we may just as well ignore the factor $(1-s/L)^2$ in (16) and adapt (14) to the present case by writing

$$\begin{aligned} r_{LB}^2(Z) &= r_{LB}^2(0)\, F'(Z) \\ F'(Z) &= \frac{3}{Z} \int_0^Z dz\, \exp(-2z/h)(1+z/z_o)^{-2/3}[1+(z+z_o)/\ell_s]^{-2/3} \end{aligned} \tag{19}$$

We have utilized $L\sin\theta = Z$ in this formula, as in the previous section. The numerical work is a little more complex than in Section II.

(i) *Dawn, dusk*: In this case (17) simplifies to

$$F'(Z) = \frac{3z_o}{Z} \int_1^{Z/z_o} dx\, (1+x)^{-2/3}\, \exp(-2xZ/h), \tag{20}$$

and when $Z \ll h/2$ (we need not consider the other case because the model is then too uncertain) it follows that, to good approximation,

$$F'(Z) \sim 9(z_o/Z)^{2/3} \text{ for } Z \ll h/2. \tag{21}$$

(ii) *Sunny day-midday*: To sufficiently accurate approximation, (19) can be simplified to

$$F'(Z) \approx \frac{3 z_o^{1/3} \ell_s^{2/3}}{Z} \int_1^{Z/z_o} dx\, x^{-2/3}(1+x)^{-2/3} \exp(-2xz_o/h), \tag{22}$$

and a further approximation is to replace Z/z_o in the upper bound of integration by ∞. Replacing x by y-1/2, we obtain an integrand $(y^2-1)^{-2/3}$, in which we may ignore the -1 term; i.e.,

$$F'(Z) \sim \frac{3 z_o^{1/3} \ell_s^{2/3}}{Z} \int_{3/2}^{\infty} dy\, y^{-4/3} \sim 9\, z_o^{1/3} \ell_s^{2/3} / Z. \qquad (23)$$

The resulting expressions (21) and (23) are inserted into (15) which is plotted in Figure 6 for air-to-ground propagation. The effects of turbulence are somewhat larger in this case than in the equivalent opposite case: ground-to-air. The reason is that the filter factor of (12) eliminates contributions from low-altitude $C_n^2(z)$, whereas that of (16) removes high-altitude (much lower) $C_n^2(z)$. This may appear surprising, but we must remember that the focussed bundle consists of spherical wavelets leaving the aperture at $z = 0$ and coming together close to $z = L$, each at its own angle. Turbulence affects the direction of a spherical wave most when the distance from the point of transmission is large. The effect is analogous to the "dirty windshield" effect: a driver with a dirty windshield can be blinded by the headlight of an oncoming car, but the oncomer cannot see that the windshield of the other car is dirty.

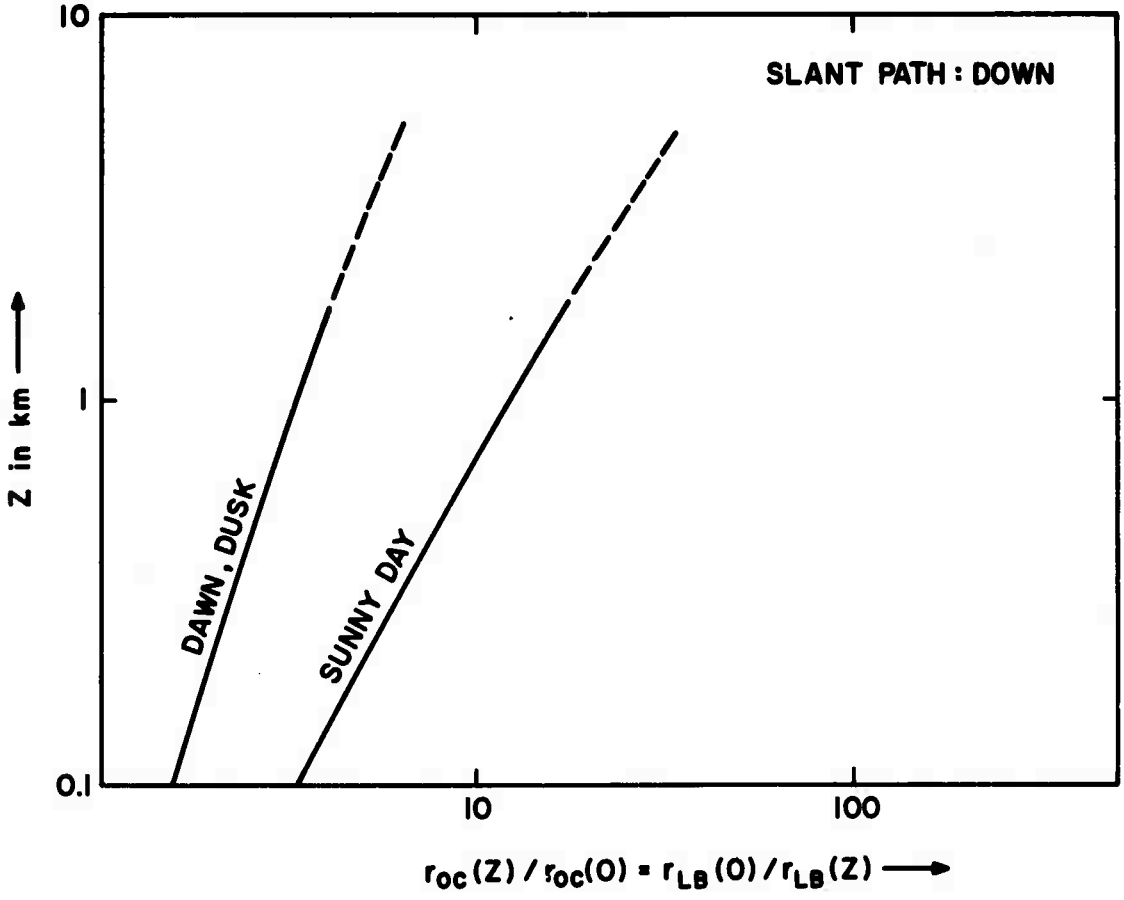

Figure 6. Modification factors for r_{Lo} and r_{oc} (from Figures 1 to 3) for air-to-ground propagation for laser transmitters at altitude Z.

IV. SCINTILLATION RATES: ANGULAR-FLUCTUATION POWER SPECTRUM

A. INTRODUCTION

So far, we have discussed only the *average* focal-spot broadening due to atmospheric turbulence. What really happens is that the focal spot *scintillates* around the average. Consequently the next questions deal with higher-order statistics such as the variance of the focal-spot area around the mean, and with the time scales on which this phenomenon occurs.

We will occupy ourselves in this section with the time scale of scintillation; i.e., with scintillation rates. There are many ways to define a significant measure of scintillation rates, but the one most commonly used is the *power spectrum* of a scintillating quantity. The power spectrum is the Fourier transform (with respect to separation time τ) of the autocovariance of the scintillating quantity with itself at a time τ later. It is a function of the conjugate variable ω, an angular frequency.

Let us try to define an appropriate autocovariance function $R_{LB}(\tau)$ that reduces to r_{LB}^2 when $\tau \to 0$. To do so, we note that the average of Equation (A-1) is a special case of

$$\begin{aligned} &\langle E(\vec{r};t)E^*(\vec{r};t+\tau)\rangle \\ &\propto \int d^2\rho_1 \int d^2\rho_2 \, \langle B(\vec{r},\vec{r}_1;t)B^*(\vec{r},\vec{r}_2;t+\tau)\rangle U_o(\vec{r}_1)U_o^*(\vec{r}_2)\exp[ik\vec{\rho}\cdot(\vec{\rho}_1-\vec{\rho}_2)/L]. \end{aligned} \tag{24}$$

When $\tau \to 0$, we note that the above formula reduces to that for $\langle I(\vec{r})\rangle$. So the new definition that we introduce for $R_{LB}(\tau)$ is obtained from (5) by replacing $\langle I(\vec{\rho},L)\rangle$ in the numerator by (24), viz.,

$$R_{LB}(\tau) = \int_0^\infty d^2\rho\rho^2[\langle E(\vec{r};t)E^*(\vec{r};t+\tau)\rangle - I_o(\vec{r})] \Big/ \int_0^\infty d^2\rho \langle I(\vec{r})\rangle , \tag{25}$$

where $\vec{r} = (\vec{\rho},L)$. In fact, the numerator of this definition can be obtained by multiplying $\rho\,[E(\vec{r};t)-E_o(\vec{r};t)]$ by the complex conjugate of $\rho\,[E(\vec{r};t+\tau)-E_o(\vec{r};t+t)]$, averaging this and then integrating over the focal plane (the cross terms are zero on the average). It is therefore plausible that $R(\tau)$ is physically analogous to the autocovariance of a focal-spot radius at time separation τ. Let us therefore adopt (25) as the desired autocovariance.

If the derivation in Appendix I is followed with this one difference: (24) is to be used instead of (A-2), it is readily seen that we obtain, instead of (A-10),

$$R_{LB}(\tau) = \frac{L^3 \epsilon^2}{24\pi} \int_0^\infty dK K^3 \Phi_4(K;\tau), \tag{26}$$

where $\epsilon^2 \Phi_4(K;\tau)$ is the Fourier transform of $< \delta\epsilon(\vec{r}_1;t)\delta\epsilon(\vec{r}_2;t+\tau) >$ averaged also over t, with respect to the difference coordinate $\vec{r}_1 - \vec{r}_2 = \Delta\vec{r}$. It will be noted by comparing (26) with Appendix II of Reference [1] that

$$R_{LB}(\tau) = \frac{L^2}{3} < \delta\vec{\theta}(t) \cdot \delta\vec{\theta}(t+\tau) > , \tag{27}$$

i.e., that the autocovariance of a weighted focal-spot radius is intimately associated with the autocorrelation of the angular deviation $\delta\vec{\theta}$ of a ray over a path of length L. For those who feel uncomfortable with the definition given for $R_{LB}(\tau)$, we can therefore state that another physical interpretation of this quantity is that it is proportional to the autocovariance of the angular deviation of a ray. Let us therefore define

$$\begin{aligned} R_\theta(\tau) &\equiv < \delta\vec{\theta}(t) \cdot \delta\vec{\theta}(t+\tau) > \\ &= \frac{L\epsilon^2}{16\pi} \int d^2K K^2 \Phi_4(K;\tau). \end{aligned} \tag{28}$$

The connection between R_θ and R_{LB} follows from (27). We shall now restrict ourselves to (28), and to horizontal propagation with uniform C_n^2 along the path for simplicity. Extensions to slant paths will be pointed out where germane.

The major point in further developing (28) is to make a good hypothesis for $\Phi_4(K;\tau)$. By definition

$$\Phi_4(K;\tau) \equiv \int d^3\Delta r \; < \delta\epsilon(\vec{r}_1;t) \; \delta\epsilon^*(\vec{r}_2;t+\tau) > \; e^{i\vec{K}\cdot\Delta\vec{r}}, \tag{29}$$

where averaging over time is implied. In Appendix II, we utilize Favre's hypothesis[8] to find (A-17) as the major step in ensuing development. Inserting (A-17) into (28), one obtains,

$$R_\theta(\tau) = \frac{L\epsilon^2}{8\pi} \int_0^\infty dK K^3 \Phi(K) \; J_o(KU_T \tau) \; \exp(-\frac{4}{3} K^2 \Delta U^2 \tau^2), \tag{30}$$

where U_T is the component of the mean velocity normal to the propagation direction, and ΔU^2 is the variance of the wind velocity in isotropic turbulence. When $\Delta U^2 = 0$, Equation (28) describes "frozen flow" or "Taylor's hypothesis": the motion is a steady convection of a random spatial structure of eddies (that are immobile with respect to each other) across the beam with velocity

component U_T. By using Equation I-3 of Reference [1], and transforming K to a new variable $x = K^2 L_o^2$, we rewrite (30) as

$$R_\theta(\tau) = \frac{15.7}{16\pi} \cdot \frac{\epsilon^2 L}{L_o} \int_0^\infty dx x(1+x)^{-11/6} J_o(\omega_T \tau \sqrt{x}) \times \exp[-x(\Delta\omega^2 \tau^2/4 + 1/\kappa_m^2 L_o^2)], \tag{31}$$

where $\omega_T = U_T/L_o$ and $\Delta\omega^2 = 16\Delta U^2/3L_o^2$ are the frequencies obtained by dividing the previously introduced velocities by the macroscale L_o. Finally, the *power spectrum* of angular fluctuations, $W_\theta(\omega)$, is the Fourier transform of (31):

$$W_\theta(\omega) \equiv 2 \int_0^\infty d\tau \, R_\theta(\tau) \cos \omega\tau \tag{32}$$

A simplification can be made by noting that $x(1+x)^{-11/6} = (1+x)^{-5/6} - (1+x)^{-11/6}$. It allows one to rewrite (31) and (32) as

$$W_\theta(\omega) = \frac{15.7}{8\pi} \cdot \frac{\epsilon^2 L}{L_o} [W_\theta(\omega, 5/6) - W_\theta(\omega, 11/6)], \tag{33}$$

with the following definition of $W_\theta(\omega,q)$:

$$W_\theta(\omega,q) = \int_0^\infty d\tau \int_0^\infty dx \, (1+x)^{-q} J_o(\omega_T \tau \sqrt{x}) \times \exp[-x(\Delta\omega^2 \tau^2/4 + 1/\kappa_m^2 L_o^2)] \cos \omega\tau. \tag{34}$$

Thus, we attempt to compute (34) for $q = 5/6$ and for $q = 11/6$, and insert the difference into (33) to obtain the power spectrum. Unfortunately, the double integral in (34) does not appear integrable into a tabulated function in general. However, we can do two special cases, namely $\Delta\omega = 0$ and $\omega_T = 0$. These two cases are the subject of subsections B and C.

B. FROZEN FLOW (TAYLOR'S HYPOTHESIS), $\Delta U^2 = 0$

In this case, it is easiest to carry out the Fourier transformation in (34) first, inverting the order of integration, to obtain

$$W_\theta(\omega,q) = \int_{\omega^2/\omega_T^2}^\infty dx \, (1+x)^{-q} (x\omega_T^2 - \omega^2)^{-1/2} \exp(-x/\kappa_m^2 L_o^2). \tag{35}$$

Let us also introduce the frequency $\Omega_T = \kappa_m U_T$; it corresponds to a velocity divided by a microscale. Equation (35) is easily transformed into,

$$W_\theta(\omega,q) = \omega_T^{2q-2}\, e^{-\omega^2/\Omega_T^2} \int_0^\infty dy\, y^{-1/2}(y+\omega^2+\omega_T^2)^{-q}\, e^{-y/\Omega_T^2}$$

$$= \frac{\sqrt{\pi}}{\omega_T}\left(1+\frac{\omega^2}{\omega_T^2}\right)^{1/2-q} e^{-\omega^2/\Omega_T^2}\, U\left(\frac{1}{2},\ \frac{3}{2}-q,\ \frac{\omega^2+\omega_T^2}{\Omega_T^2}\right) . \tag{36a}$$

The second form was obtained by utilizing Equation (14.4.12) of Reference [9], and converting the Whittaker function in the result to a Kummer function U(a,b,z) as in Equation (13.1.33) of Reference [10]. Let us see what $W_\theta(\omega,q)$ looks like for different parameter regimes:

(i) $\omega << \Omega_T$:

For the case that ω is much less than the microscale-defined frequency $\Omega_T \sim U_T/\ell_o$, we can utilize Equations (13.5.10) and (13.5.12) of Reference [10] to obtain

$$W_\theta(\omega,q) \approx \frac{\Gamma(q-1/2)}{\Gamma(q)} \cdot \frac{\sqrt{\pi}}{\omega_T}\left(1+\frac{\omega^2}{\omega_T^2}\right)^{1/2-q} \tag{36b}$$

(ii) $\omega >> \Omega_T$:

In this case, we utilize the asymptotic form of Kummer's function $U(a,b,z) \to z^{-a}$ to find,

$$W_\theta(\omega,q) \quad \kappa_m L_o \frac{\sqrt{\pi}}{\omega_T}\left(1+\frac{\omega^2}{\omega_T^2}\right)^{-q} e^{-\omega^2/\Omega_T^2} . \tag{36c}$$

This formula is not very interesting since $\omega >> \Omega_T$ implies a strong Gaussian decay factor making (36c) quite negligible compared to (36b).

Note that the power spectrum is flat below $\omega \approx U_T/L_o$, and then decays as $\omega^{-2/3}$ for $U_T/L_o < \omega << U_L/\ell_o$. As ω approaches U_T/ℓ_o, the decay sharpens into a Gaussian cut-off, but this has as much meaning as the Gaussian cut-off in $\Phi(K)$.

C. RANDOM VELOCITY (NO MEAN), $U_T = 0$

Returning to (34), we again carry out the Fourier transformation first to obtain,

$$W_\theta(\omega,q) = \frac{\sqrt{\pi}}{\Delta\omega}\int_0^\infty dx x^{-1/2}(1+x)^{-q}\exp\left[-\left(\frac{\omega^2}{x\Delta\omega^2} - \frac{x}{\kappa_m^2 L_o^2}\right)\right]. \tag{37}$$

This case is slightly harder to handle than the previous one. We can drop the $x/\kappa_m^2 L_o^2$ term in the exponential because the first term in it will take care of convergence. With the simplification, we set $x = 1/y$ in (37) to obtain

$$W_\theta(\omega,q) \approx \frac{\sqrt{\pi}}{\Delta\omega}\int_0^\infty dy y^{q-3/2}(1+y)^{-q}\exp(-y\omega^2/\Delta\omega^2)$$
$$= \Gamma(q-1/2)\frac{\sqrt{\pi}}{\Delta\omega}U\left(q-\frac{1}{2},\frac{1}{2},\frac{\omega^2}{\Delta\omega^2}\right). \tag{38a}$$

The development of the second form is the same as that in (36a). It can be seen that the general shape is similar to (36b) by using the asymptotic forms of the Kummer function in (38a):

$$W_\theta(\omega,q) \sim \frac{\Gamma(q-1/2)}{\Gamma(q)}\frac{\pi}{\Delta\omega} \text{ for } \omega << \Delta\omega,$$
$$\sim \Gamma(q-1/2)\frac{\sqrt{\pi}}{\Delta\omega}\left(\frac{\omega}{\Delta\omega}\right)^{1-2q} \text{ for } \omega >> \omega. \tag{38b}$$

We can also develop another form from (37) for $\omega >> \Delta\omega$ by retaining the $\exp(-x/\kappa_m^2 L_o^2)$ but setting $(1+x)^{-q} \approx x^{-q}$. Equation (37) is then reduced by utilizing the Laplace transform (4.5.29) of Reference [9], and by introducing the microscale-governed frequency $\Delta\Omega^2 = 16\kappa_m^2\Delta U^2/3$. We obtain (for $q > 1/2$),

$$W_\theta(\omega,q) = \frac{2\sqrt{\pi}}{\Delta\omega}\left(\frac{\kappa_m L_o\omega}{\Delta\omega}\right)^{1/2-q}K_{q-1/2}(2\omega/\Delta\Omega)$$
$$\sim \Gamma(q-1/2)\frac{\sqrt{\pi}}{\Delta\omega}\left(\frac{\omega}{\Delta\omega}\right)^{1-2q} \text{ for } \omega << \Delta\Omega \tag{38c}$$
$$\sim (\kappa_m L_o)\frac{\pi}{\Delta\omega}\left(\frac{2\omega}{\Delta\Omega}\right)^{-q}\exp(-2\omega/\Delta\Omega) \text{ for } \omega >> \Delta\Omega.$$

Here, $K_{q-1/2}(2\omega/\Delta\Omega)$ is a modified Bessel function in the notation of Reference [10], and the two asymptotic forms are easily obtained. We note that the second form in (38c) agrees with the second form in (38b) thus confirming the validity of the approximations. It is also clear that the power spectrum cuts off abruptly as ω approaches and exceeds $\Delta\Omega \sim \Delta U/\ell_o$.

Just as in case B, we note that the power spectrum starts off flat below $\omega \approx \Delta U/L_o$, and then it decays as $\omega^{-2/3}$ until the cut-off at $\omega \approx \Delta U/\ell_o$.

D. SUMMARIZED RESULTS AND APPROXIMATED POWER SPECTRUM FOR GENERAL CASE

The results found in this section amount to the following. We assume a random velocity distribution with mean U_o and variance ΔU^2. The component of mean velocity across the beam is U_T. We have defined a power spectrum of focal-spot radius fluctuations that is proportional to the power spectrum of angular fluctuations. The latter is named $W_\theta(\omega)$. It has to be a function of U_T and ΔU^2. We have defined some frequencies by dividing these velocities by length scales:

$$\omega_T = U_T/L_o \quad , \quad \Delta\omega^2 = 16\Delta U^2/3L_o^2$$
$$\Omega_T = \kappa_m U_T \quad , \quad \Delta\Omega^2 = 16\kappa_m^2\Delta U^2/3 \ . \tag{39}$$

Furthermore, we have found that $W_\theta(\omega)$ is the difference of two parts, see Equation (33). In Tables I and II we summarize the results for $W_\theta(\omega,q)$, bearing in mind that we subtract the $q = 11/6$ equations from the $q = 5/6$ ones to get the power spectrum.

It is interesting to compare the random-flow with the frozen-flow results. The spectra are very similar. We would like to suggest an approximate formula for engineering purposes. To do so, we note from (31) two properties:

$$R_\theta(0) = \frac{1}{\pi}\int_0^\infty d\omega W_\theta(\omega) = \frac{15.7}{16\pi}\ \frac{\epsilon^2 L}{L_o}\ \Gamma(11/6)\ (\kappa_m L_o)^{1/3},$$
$$-\left[\frac{\partial^2 R_\theta(\tau)}{\partial\tau^2}\right]_{\tau=0} = \frac{1}{\pi}\int_0^\infty d\omega\omega^2 W_\theta(\omega) = \frac{15.7}{16\pi}\cdot\frac{\epsilon^2 L}{L_o}\cdot\frac{\Gamma(7/6)}{2}\ (\kappa_m L_o)^{7/3}\ (\omega_T^2+\Delta\omega^2). \tag{40}$$

The second property expresses the variance width of the power spectrum. It is equal to the mean square width because $W_\theta(\omega)$ is symmetric around $\omega = 0$ so that we utilize cosine transforms in the preceding. The first property simply recalculates the angular-fluctuation variance and states that it is the zeroth moment of $W_\theta(\omega)$. The interesting point is that (40) is a function of $\omega_T^2+\Delta\omega^2$. We already know that the flat part of $W_\theta(\omega)$ (for $\omega < \omega_T, \Delta\omega$) does not contribute appreciably to $R_\theta(0)$ because it can be seen readily from (31) if we set $1+x = x$

TABLE I

Frozen Flow ($\Delta U=0$)

$W_\theta(\omega,q)$

$\frac{\sqrt{\pi}}{\omega_T}\left(1+\omega^2/\omega_T^2\right)^{1/2-q} e^{-\omega^2/\Omega_T^2}\ U[1/2,\ 3/2-q,\ (\omega^2+\omega_T^2)/\Omega_T^2)]$		
$\frac{\Gamma(q-1/2)}{\Gamma(q)}\frac{\sqrt{\pi}}{\omega_T}\left(1+\omega^2/\omega_T^2\right)^{1/2-q} e^{-\omega^2/\Omega_T^2}$		$\frac{\sqrt{\pi}}{\omega_T}\frac{\Omega_T}{\omega_T}(1+\omega^2/\omega_T^2)^{-q} e^{-\omega^2/\Omega_T^2}$
$\frac{\Gamma(q-1/2)}{\Gamma(q)}\frac{\sqrt{\pi}}{\omega_T}$	$\frac{\Gamma(q-1/2)}{\Gamma(q)}\frac{\sqrt{\pi}}{\omega_T}\left(\frac{\omega}{\omega_T}\right)^{1-2q}$	$(\kappa_m L_o)\frac{\sqrt{\pi}}{\omega_T}\left(\frac{\omega}{\omega_T}\right)^{-2q} e^{-\omega^2/\Omega_T^2}$

$\omega_T = U_T/L_o$ $\qquad$ $\Omega_T = \kappa_m U_T$ $\qquad$ $\omega \rightarrow$

TABLE II

Random flow ($U_T - 0$)

$W_\theta(\omega,q)$

	$\frac{\sqrt{\pi}}{\Delta\omega}\ \Gamma(q-1/2)\ U(q-1/2,\ 1/2\ \omega^2/\Delta\omega^2)$	
	$\frac{\sqrt{\pi}}{\Delta\omega}\ 2(\kappa_m L_o \omega/\Delta\omega)^{1/2-q}\ K_{q-1/2}\ (2\omega/\Delta\Omega)$	
$\frac{\Gamma\ (q-1/2)}{\Gamma\ (q)}\ \frac{\Pi}{\Delta\omega}$	$\Gamma\ (q-1/2)\left(\frac{\sqrt{\pi}}{\Delta\omega}\right)^{1-2q}\ \frac{\omega}{\Delta\omega}$	$(\kappa_m L_o)\ \frac{\pi}{\Delta\omega}\left(\frac{2\omega}{\Delta\Omega}\right)^{-q}\ e^{-2\omega/\Delta\Omega}$

$\Delta\omega \sim \Delta U/L_o$ $\qquad$ $\Delta\Omega \sim \kappa_m \Delta U$ $\qquad$ $\omega \rightarrow$

that the resulting power spectrum then has no flat part, and we have already seen that this is a valid approximation in computing $R_\theta(0)$. Consequently, the flat part is even less important in computing the second of (40). Since most of the area under $W_\theta(\omega)$ lies in the $\omega^{-2/3}$ portion ($q = 5/6$ yields an $\omega^{-2/3}$ behavior that dominates over the $q = 11/6$, $\omega^{-8/3}$ part), it appears to us that this portion of the curve is governed by a parameter $\omega^2/(\omega_T^2+\Delta\omega^2)$. Consequently, we suggest that the following formula is useful over the entire range of ω:

$$W_\theta(\omega) = \frac{15.7}{8\pi}\frac{\epsilon^2 L}{L_o}\left[W_\theta(\omega,5/6) - W_\theta(\omega,11/6)\right],$$

$$W_\theta(\omega,q) = \left(\frac{\pi}{\omega_T^2+\Delta\omega^2}\right)^{1/2}\left(1+\frac{\omega^2}{\omega_T^2+\Delta\omega^2}\right)^{1/2-q}\exp\left[-\omega^2/(\Omega_T^2+\Delta\Omega^2)\right], \tag{41a}$$

$$\times\, U\left[1/2,\ 3/2-q,\ (\omega^2+\omega_T^2+\Delta\omega^2)/(\Omega_T^2+\Delta\Omega^2)\right] .$$

This formula clearly satisfies (40) because it reduces to (36a) if we set $\Delta\omega = 0$, and (36a) yields (40) with $\Delta\omega = 0$. It is obvious that by substituting $\omega_T^2+\Delta\omega^2$ for ω_T^2 in (36a) we satisfy (40) in general, and we obtain the above formula (41). When $\omega^2 << \Omega_T^2+\Delta\Omega^2$, we can utilize the approximation

$$W_\theta(\omega,q) \approx \frac{\Gamma(q-1/2)}{\Gamma(q)}\left(\frac{\pi}{\omega_T^2+\Delta\omega^2}\right)^{1/2}\left(1+\frac{\omega^2}{\omega_T^2+\Delta\omega^2}\right)^{1/2-q} \tag{41b}$$

Comparing (41b) to the results in Tables I and II, we note that we obtain the previous results to reasonable approximation. If we allow $\omega_T \to 0$, we note that the (41b) approximation is in error for $\omega << \Delta\omega$ by a factor $\sqrt{\pi}$, and by a factor $\Gamma(5/6) \approx 1.1$ for $\omega >> \Delta\omega$. This appears sufficient for engineering purposes. Furthermore, (41b) is in error when $\omega_T \to 0$ for $\omega \gtrsim \Delta\Omega$, but here the spectrum is very small and its precise shape is governed by the dissipation range of turbulence for which the precise shape is not crucial anyway. By choosing (41) as we have, we at least assure ourselves of the proper normalizations (40) although the cut-off shape at $\omega \sim \Delta\Omega$ is not described properly. The transition regions are probably also imprecise.

Therefore, in conclusion it appears to us that the power spectrum of angular fluctuations, hence that of focal-spot scintillation, is adequately described by (41). That is to say,

(i) the spectrum is flat for $\omega < (\omega_T^2+\Delta\omega^2)$.

(ii) it falls off as $[\omega^2/(\omega_T^2+\Delta\omega^2)]^{-1/3}$

for $(\omega_T^2+\Delta\omega^2)^{1/2} < \omega < (\Omega_T^2+\Delta\Omega^2)^{1/2}$.

(iii) it cuts off sharply beyond $\omega = (\Omega_T^2+\Delta\Omega^2)^{1/2}$.

To our knowledge, no calculations of $W_\theta(\omega)$ exist in the literature for this general case. However, Lawrence and Strohbehn[11] cite untranslated work by A. S. Gurvich, M. A. Kallistratova, and N. S. Time (Izv. Vyssh. Ucheb. Zaved. Radiofizika 11, pp. 1360-1370, 1968) for the Taylor's hypothesis case ($\Delta\omega = 0$). Figure 10 of Reference [11] shows a plot of essentially $\omega W_\theta(\omega)$ vs. ω which appears to be misinterpreted in the text of Reference [11]. All three portions (i) - (iii) of the behavior mentioned above are borne out by this graph which appears to us to correspond to $\omega_T \sim 1$ Hz (note that $\omega_T = 2\pi f_T$), and $\Omega_T \sim 300$ Hz (because the peak of the curve is at $\kappa_m L_o f_T \approx 50$ Hz).

APPENDIX I

THE VARIANCE-WIDTH THEOREM FOR FOCAL-SPOT AREA

The purpose of this Appendix is to derive (3) in a very general fashion and to stress the approximations in it. These do not appear to be understood as clearly as is desirable in context with the derivation in Reference[1].

Referring for notation to Reference[1], and specifically to Section III, we note that the irradiance in the focal plane (for a focussed laser beam) is,

$$I(\vec{r}) \propto \left| \int d^2\rho_1 \; B(\vec{r},\vec{r}_1)\; U_o(\vec{r}_1)\; \exp(ik\,\vec{\rho}\cdot\vec{\rho}_1/L) \right|^2 \qquad \text{(A-1)}$$

Here, $U_o(\vec{r}_1)$ is the transmittance amplitude, the so-called pupil function, of the aperture at $z = 0$, and coordinate $\vec{r}_1 = (\vec{\rho}_1 0)$. Previously, U_o was chosen to be Gaussian. At present, it can be considered any generally accepted shape. The "sharp-beam" choice $U_o(\vec{r}_1) = 1$ for $\rho_1 \leq r_o$, and zero otherwise, yields the Airy disk in (A-1) when there are no atmospheric effects ($B = 1$).

The approximations in (A-1) are:

(i) radiation-zone, $kL >> 1$
(ii) near field of the aperture, $L << kr_o^2$
(iii) sagittal, $kr_o^4 << L^3$

These are not very great restrictions at all for $\lambda = 10.6$ μm and higher-frequency propagation. At 10.6 μm, one finds $kr_o^2 \sim 100$ km, and $(kr_o^4)^{1/3} \sim 30$ m. Clearly 1 km < L < 10 km yields correction terms to (A-1) that are quite small.

To proceed further, we note that the expression inside modulus bars in (A-1) is a two-dimensional Fourier transform of a function of $\vec{\rho}_1$. The conjugate variable is $k\vec{\rho}/L = \vec{q}$, and consequently the irradiance is a function of L and of $\vec{q}$. Therefore

$$I(\vec{q}) \propto \left| \int d^2\rho_1 \; B(\vec{r},\vec{r}_1)\; U_o(\vec{r}_1)\; \exp(i\vec{q}\cdot\vec{\rho}_1) \right|^2. \qquad \text{(A-2)}$$

When $B(\vec{r},\vec{r}_1) = 1$, we obtain $I_o(\vec{q})$, the free-space irradiance pattern in the focal plane $z = L$.

Only one more approximation will be made: it is assumed that every vector $\vec{r}-\vec{r}_1$ for $|\vec{r}-\vec{r}_1| \lesssim r_o$ is perpendicular to the plane $z = 0$. This yields,

(iv) small-angle approximation, $r_o << L$

This approximation yields extremely small errors and is easily satisfied in all practical situations. It is needed only so that $\langle B(\vec{r},\vec{r}_1)B^*(\vec{r},\vec{r}_2)\rangle$ can be replaced by the mutual-coherence function (mcf) with axis $\vec{r} \perp \vec{r}_1-\vec{r}_2$.

Because $\langle B(\vec{r},\vec{r}_1)B^*(\vec{r},\vec{r}_2)\rangle$ is a function of the difference coordinate $\vec{\Delta\rho} = \vec{r}_1-\vec{r}_2$, a Fourier-transform pattern $I_B(\vec{q})$ can be defined as follows

$$\langle I_B(\vec{q}) \equiv \int d^2\Delta\rho \langle B(\vec{r},\vec{r}_1)\ B^*(\vec{r},\vec{r}_2)\rangle\ \exp(i\vec{q}\cdot\vec{\Delta\rho}). \tag{A-3}$$

The average of Equation (A-2) can be rewritten as a convolution integral of I_B and I_o because of this property of the mcf of the normalized spherical-wave field B:

$$\langle I_B(\vec{q})\rangle = \frac{1}{4\pi^2}\int d^2q_1\ I_o(\vec{q}_1)\ I_B(\vec{q}-\vec{q}_1). \tag{A-4}$$

This formula for the average irradiance is not new, but it is useful to stress its convolution property. It states that the free-space irradiance pattern $I_o(\vec{q})$ is broadened by the pattern $I_B(\vec{q})$ which depends only upon the mcf of normalized spherical-wave fields in turbulent air.

We now define variance widths for $\langle I\rangle$, I_o, and I_B, namely σ^2, σ_o^2, and σ_B^2 respectively:

$$\sigma^2 \equiv \frac{\int d^2q\ q^2\ \langle I(\vec{q})\rangle}{\int d^2q\ \langle I(\vec{q})\rangle} - \left[\frac{\int d^2q\ q\ \langle I(\vec{q})\rangle}{\int d^2q\ \langle I(\vec{q})\rangle}\right]^2. \tag{A-5}$$

Likewise, definitions for σ_o^2 and σ_B^2 can be written down, although omitted here. If (A-4) is inserted into numerators and denominators of (A-5), one finds the variance-width theorem after some rearrangement of terms:

$$\sigma^2 = \sigma_o^2 + \sigma_B^2 \tag{A-6}$$

Note that the derivation depends only upon the validity of (A-2), which requires assumptions (i)-(iii) and the fact that the mcf $\langle B(1)B^*(2)\rangle$ (in shorthand notation) is a function of $\vec{r}_1-\vec{r}_2$. In applying (A-6) to effective irradiance-pattern widths, it is also noted that each σ^2 need be divided by $(k/L)^2$ to yield actual widths. Thus, if we define $r_L = (L/k)\sigma$, $r_{Lo} = (L/k)\sigma_o$, and $r_{LB} = (L/k)\sigma_B$, we obtain

$$r_L^2 = r_{Lo}^2 + r_{LB}^2. \tag{A-7}$$

For cylindrically symmetric beams $\vec{q}I_o(\vec{q})$ is anti-symmetric with respect to the origin, hence the first moment of $I_o(\vec{q})$ is zero. The same holds for the first moment of $I_B(\vec{q})$. Hence r_L^2 is properly defined by (1), and r_{Lo}^2, r_{LB}^2 are defined likewise by replacing $< I(\vec{\rho},L) >$ by $I_o(\vec{\rho},L)$ and $I_B(\vec{\rho},L) = I_B(\vec{q})$ respectively. Finally, it is noted that an expression for r_{LB}^2 is readily obtained from the definition,

$$r_{LB}^2 = \int d^2\rho\ \rho^2\ I_B(\vec{q}) \Big/ \int d^2\rho\ I_B(\vec{q}), \tag{A-8}$$

by utilizing Equation (10) of Reference[1] for the mcf. Unfortunately, part of the exponent in that equation is in error. The correct form for $< B(1)B^*(2) >$ with $\vec{\rho} = \vec{r}_1 - \vec{r}_2$ is,

$$< B(1)B^*(2) > = \exp\left\{ - \frac{k^2 L\, \epsilon^2}{8\pi} \int_0^\infty dK K \Phi(K) \left[1 - \int_0^1 dz\ J_o(Kz\rho) \right] \right\} \tag{A-9}$$

When this is inserted into the definition of $I_B(\vec{q})$, which is then inserted in turn into (A-8), one obtains via a development analogous to that in Section IV of Reference[1],

$$r_{LB}^2 = \frac{L^3\, \epsilon^2}{24\pi} \int_0^\infty dK K^3 \Phi(K) \approx 1.3\, L^3 \kappa_m^{1/3}\, C_n^2. \tag{A-10}$$

APPENDIX II

THE RANDOM-VELOCITY HYPOTHESIS

The difficulty in (29) is that the autocovariance $<\delta\varepsilon\ (r_1;t)\ \delta\varepsilon^*(\vec{r}_2;t+\tau)>$ depends on the time separation τ. We will discuss a simple hypothesis that enables us to relate this autocovariance to the $\tau = 0$ case. Consider $\delta\varepsilon(\vec{r};t)$ in turbulent air, it is proportional to the air-density fluctuation $\delta N(\vec{r},t)$. The continuity equation states that

$$dN/dt + N\vec{\nabla}\cdot\vec{U} = 0 \tag{A-11}$$

where $N = N_o + \delta N$, and $\vec{U}$ is the gas velocity. Thus (A-11) describes the time change of δN because we may assume that $dN_o/dt = 0$. In a hydrodynamical description, both δN and $\vec{U}$ are functions of $\vec{r}$ and t, and $dN/dt = \partial N/\partial t + \vec{U}\cdot\vec{\nabla}N$. The second term of (A-11) is related to expansion or compression of the gas and the first term simply expresses conservation of density in a unit parcel of air as it flows from one location to another (perhaps changing its shape).

If we assume that "sources" of turbulence do not lie directly in or close to the propagation path, then we may assume $N\vec{\nabla}\cdot\vec{U} \approx 0$ and consider the turbulence adequately described by $dN/dt = 0$, i.e., by flow governed by a wind-velocity vector $\vec{U}(\vec{r},t)$. It is probably not a very wrong assumption to thus ignore compression and expansion of the gas, and it simplifies matters because it implies that $\delta N(\vec{r},t)$ can be written in general as

$$\delta N(\vec{r},t) = \delta N(\vec{r} + \int_t^{t+\tau} dt'\ \vec{U}(\vec{r},t'),t) \tag{A-12}$$

and similarly for $\delta\varepsilon \propto \delta N$. It is easily seen that (A-12) implies $dN/dt = 0$ by allowing $\tau \to 0$ and keeping the first-order Taylor-series terms. These yield $\partial\delta N/\partial t + U\cdot\vec{\nabla}\delta N = 0$ which is identical to $dN/dt = 0$ because N_o does not vary. We can apply (A-12) to (29) to obtain:

$$\delta\varepsilon(\vec{r}_2;\ t+\tau) = \delta\varepsilon(\vec{r}_2 - \int_t^{t+\tau} dt'\ \vec{U}(\vec{r}_2,t');\ t) \tag{A-13}$$

If this is inserted into (29) we obtain after a coordinate transformation:

$$\Phi_4(\vec{K};\tau) = <\int d^3\Delta r'\delta\varepsilon(\vec{r}_1';t)\ \delta\varepsilon_2';t)\ e^{\left[i\vec{K}\cdot\Delta\vec{r}' + \int_t^{t+\tau} dt'\ \vec{U}(\vec{r}_2,t')\right]}> \tag{A-14}$$

where $\Delta\vec{r}' = \vec{r}_1' - \vec{r}_2'$, $\vec{r}_1' = \vec{r}_1$, and $\vec{r}_2'$ is the spatial coordinate in the right-hand side of (A-13). The coordinate $\Delta\vec{r}'$ is time-dependent, but since that time dependence shows up only in the boundaries of integration, effectively replaced by $\pm\infty$ in all dimensions, we can disregard it.

The cardinal assumption to be made at this point is that the velocity structure is statistically independent of the spatial structure of $\delta\varepsilon$. It allows us to write

$$\Phi_4(K;\tau) = \int d^3\Delta r' \, \langle \delta\varepsilon(\vec{r}_1')\delta\varepsilon^*(\vec{r}_2')\rangle \, e^{i\vec{K}\cdot\Delta\vec{r}'} \left\langle e^{i\vec{K}\cdot\int_t^{t+\tau} dt'\vec{U}(\vec{r}_2,t')} \right\rangle \tag{A-15}$$

$$= \Phi(K) \left\langle \exp\left[i\vec{K}\cdot\int_t^{t+\tau} dt' \, U(t') \right] \right\rangle .$$

The space dependence of $\vec{U}$ has not been written down in the last form because an ensemble average over space and time is implied by the brackets. It is also plausible that $\vec{U}(t')$ does not vary locally very much with t' in a time interval $\tau \lesssim 1$ sec., or τ less than some other short time in which $\Phi_4(K;\tau)$ is essentially zero. Furthermore, velocity $\vec{U}$ is most likely to consist of a steady wind component and a random component, i.e., its distribution is probably adequately described by a Gaussian with non-zero mean. These two statements imply,

$$\left\langle \exp\left[i\vec{K}\cdot\int_t^{t+\tau} dt' \, \vec{U}(t') \right] \right\rangle \tag{A-16}$$

$$= e^{i\vec{K}\cdot\vec{U}_o\tau} \exp(-2K^2\Delta U_T^2 \, \tau^2).$$

Here, $\vec{U}_o$ is the mean compnent, and we note that only its component U_T in a plane normal to the propagation direction occurs in the first exponential. Likewise, ΔU_T^2 is the variance of wind velocity in this plane. If the wind variation is isotropic, then it follows that $\Delta U_T^2 = (2/3)\Delta U^2$. Finally, all this is summarized by inserting it into (A-16) which is inserted in turn into (A-15) to obtain

$$\Phi_4(K;\tau) = e^{i\vec{K}\cdot\vec{U}_T\tau} \exp\left(-\frac{4}{3} K^2\Delta U^2\tau^2\right) \Phi(K) \tag{A-17}$$

This set of assumptions leading to (A-17) is also known as Favre's hypothesis[8].

REFERENCES

1. D. A. de Wolf, Effects of Turbulence Instabilities on Laser Propagation, RCA Laboratories, First Quarterly Report to Rome Air Development Center, Griffiss AFB, New York, RADC-TR-71-249 (October 1971).
2. A. D. Varvatsis and M. I. Sancer, Can. J. Phys. 49, 1233 (1971).
3. R. F. Lutomirski and H. T. Yura, Appl. Opt. 10, 1652 (1971).
4. R. N. Bracewell, Handbook der Physik 54, 50 (1962).
5. J. C. Wyngaard, Y. Izumi, and S. A. Collins, Jr., J. Opt. Soc. Am. 61, 1646 (1971).
6. P. J. Titterton, J. Opt. Soc. Am. 60, 417 (1970).
7. G. W. Sutton, J. Opt. Soc. Am. 59, 115 (1969).
8. A. J. Favre, J. Appl Mech., 241 (June 1965).
9. A. Erdelyi, Ed., *Tables of Integral Transforms I & II*, Bateman Manuscript Project (McGraw-Hill, New York; 1954).
10. M. Abramowitz and I. A. Stegun, *Handbook of Mathematical Functions*, NBS Applied Mathematics Series 55 (U.S. Government Printing Office, Washington, D. C.; June 1964).
11. R. S. Lawrence and J. W. Strohbehn, Proc. IEEE 58, 1523 (1970).